npj | climate and atmospheric science

Article

Published in partnership with CECCR at King Abdulaziz University

https://doi.org/10.1038/s41612-025-01284-6

Multiple oceanic sources of alkylamines in Southern Ocean atmospheres

Manuel Dall´Osto[1,2,9] ✉, Mark F. Fitzsimons[3], James Brean[2], Preston Chebai Akenga[4], A. Jones[5], Tom Lachlan-Cope[5], Ana Sotomayor[1], Elisa Berdalet[1], Dolors Vaque[1], Roy M. Harrison[2,7], Karam Mansour[6,8], Matteo Rinaldi[6], Stefano Decesari[6], David Beddows[2] & Marco Paglione[6,9]

Measurements of pre-industrial conditions are of paramount importance for understanding historical climate change. The Southern Ocean and Antarctic continent are some of the least polluted environments on planet Earth. Alkylamines can rapidly partition into aerosols, increasing their mass, as well as form new particles altogether. We demonstrate the importance of pelagic "open ocean" (OO) and sympagic "sea ice" (SI) regions in supplying distinct organic nitrogen aerosol components. In the aerosol phase, dimethylamine (DMA) and trimethylamine (TMA) are both secondary, though DMA likely originates mainly from pelagic regions, while TMA is associated mainly with sympagic regions. Parallel measurements in ice and surface waters reveal that melting sea ice contains a factor of four more TMA than coastal Antarctic Peninsula waters; and seventeen times more TMA than OO regions - suggesting additional coastal Antarctic sources. To better interpret future climate change, we recommend employing regional atmospheric chemistry models to understand these diverse aerosol sources.

Climate change is setting our planet earth in danger, the passage beyond tipping points could lead to irreversible effects on natural systems crucial for organisms' lives, and leading to significant human societal impacts[1]. The industrial revolution has extensively increased aerosol concentrations, and the projections of aerosols and their interaction with clouds in the control of the radiation budget are highly uncertain[2].

In order to reduce such large uncertainty in estimates of radiative forcing due to human activity[3], the remote Southern Ocean (SO) is the only environment left to define a baseline for preindustrial aerosol-cloud interactions[4]. While local sources dominate, cloud condensation nuclei (CCN) and ice nucleating particle (INP) budgets and sources for the SO are not fully constrained[5]. The sources of alkylamines, nitrogen-containing organic bases which readily partition into the aerosol phase, are some of the most uncertain. Alkylamines can both contribute to the rapid formation of new particles[6,7] and enter the aerosol phase directly[8], contributing to the absorptive effect of aerosols[9].

Antarctic particle number concentrations have a strong seasonal cycle, with a maximum in the summertime[10,11], linked with biological processes occurring in the surrounding oceans. Early hypotheses argued that particle number concentrations are dictated by dimethylsulphide (DMS) emissions, and their subsequent oxidation[12]. This is opposed by a much more complex view of aerosol sources in the marine boundary layer and the subsequent response of clouds to changes in aerosol[13]. Indeed, the oversimplification of two broad natural sources governing the aerosol population in the SO region – sea spray aerosol (SSA, mostly composed of sea salt) and non-sea salt sulfate (nss-SO_4^{2-}) – has been challenged in a recent intensification in Antarctic aerosol measurement field campaigns[14–18]. Aerosol sources in sub-Antarctic and Antarctic coastal areas vary substantially, and such complexity is reflected in the difficulty of representing aerosol concentrations based on latitudinal changes. Emerging recent literature has shown that aerosol populations of variable chemical composition can be observed within polar Antarctic (>60° S) air masses. Indeed, by reporting simultaneous aerosol size distribution measurements at three sites (Halley, King Sejong and Dome C stations in Antarctic), ref. 19 showed that the dynamics of aerosol number concentrations and distributions is more complex than the simplified view of particles composed of a sulfate–sea-spray combination, and it is likely that an array of additional chemical components and processes drive the aerosol population. Aerosol sources around Antarctica

[1]Institute of Marine Sciences, CSIC, Passeig Marítim de la Barceloneta, Barcelona, Spain. [2]National Center for Atmospheric Sciences, University of Birmingham, Birmingham, United Kingdom. [3]Biogeochemistry Research Centre, Marine Institute, School of Geography, Earth and Environmental Sciences, University of Plymouth, Drake Circus, Marine Laboratory, Plymouth, United Kingdom. [4]Kisii University, Kisii, Kenya. [5]Natural Environment Research Council, British Antarctic Survey, Cambridge, UK. [6]Institute of Atmospheric Sciences and Climate, National Research Council, Bologna, Italy. [7]Present address: Department of Environmental Sciences, Centre of Excellence in Environmental Studies, King Abdulaziz University, Jeddah, Saudi Arabia. [8]Present address: Oceanography Department, Faculty of Science, Alexandria University, Alexandria, Egypt. [9]These authors contributed equally: Manuel Dall´Osto, Marco Paglione.
✉e-mail: dallosto@icm.csic.es

and the Southern Ocean are dominantly open ocean marine areas and the Antarctic continent, with minor contributions from long-range transported dust or anthropogenic material. A new hypothesis was proposed by ref. 14: what if the microbiota of sea ice and sea ice-influenced (sympagic) ocean are a significant source of atmospheric aerosols and their precursors (additional to nss-SO_4^{2-}); and are those different from pelagic open oceans and terrestrial regions? Indeed—by means of synergistic atmospheric and oceanic measurements in the sympagic Weddell Sea—evidence of atmospheric organic nitrogen, including low molecular weight alkyl-amines, was presented[14]. However, local aquatic Chlorophyll-a did not co-vary with the identified nitrogen compounds, stressing already the complexity of biogeochemical ocean-atmosphere interactions. In follow up studies[20], non-methanesulfonic acid Water-Soluble Organic Matter (non-MSA WSOM) was found to account for 6–8% and 11–22% of the aerosol PM_1 mass originated in open ocean (OO) and sea ice (SI) regions, respectively. It was reported that concentrations of mono-, di- and trimethylamine (MMA, DMA and TMA, respectively), and their precursors, the quarternary amines glycine betaine and choline, were enhanced in sympagic sea water samples relative to ice-devoid pelagic ones[21]. Measurements of ATOFMS (Aerosol Time-Of-Flight Mass Spectrometry, TSI 3800) ambient aerosols in the sympagic region indicated that the majority (75–89% by number of particles detected) of aerosol alkylamines were of secondary origin, i.e., incorporated into the aerosol after gaseous air-sea exchange[14,21,22].

Reference [23] found at least three main bioregion sources of water-soluble organic carbon (WSOC): (1) open Southern Ocean pelagic environments dominated by primary SSA mainly constituted of lipids and polyols, (2) sympagic areas in the Weddell Sea, with secondary Sulphur and Nitrogen organic compounds and (3) terrestrial land vegetation coastal areas, tentatively traced by specific sugars such as sucrose in aerosols. Collectively, these findings reveal that sympagic regions contribute uniquely to atmospheric aerosols, distinct from open ocean and terrestrial sources.

The Weddell Sea, covered by open and consolidated pack ice, is therefore a source of aerosol-phase organic nitrogen and should be considered when assessing secondary aerosol formation processes in Antarctica. Indeed, ref. 24 found that New Particle Formation (NPF) occurs frequently when air masses blow over regions of the extended sea-ice marginal zone; these air masses contain elevated concentrations of alkylamines and H_2SO_4, confirming that emissions from marine plankton and sea-ice melt play crucial roles in the creation of particles critical to regulation of the Antarctic climate. Other studies also point out other sources of newly formed particles, including possibly continental ponds[25], open ocean regions[26] and local penguin colonies[18].

In order to further elucidate aerosol sources and processes, ref. 27 reported for the first time, atmospheric measurements during a three month period (December 2018–March 2019) simultaneously made at two Antarctic research British Antarctic Survey (BAS) stations—namely Signy and Halley. Water Soluble Organic Matter (WSOM) was reported to be a major aerosol component at both sites (37 and 29% of water-soluble PM_1 on average, at Signy and Halley, respectively), and remarkable differences between pelagic (open ocean) and sympagic (influenced by sea ice) air mass histories and related primary and secondary organic aerosol sources were found.

Specifically, ref. 27 reported different types of primary and secondary marine organic aerosol types including: two primary organic aerosol (POA) types, characterized by sugars, polyols, and degradation products of lipids and associated with open-ocean and sympagic/coastal waters, respectively; two secondary organic aerosol (SOA) types, one enriched in methanesulfonic acid (MSA) and dimethylamine (DMA) and associated with pelagic waters and the other characterized by trimethylamine (TMA) and linked to sympagic environments; and a fifth component of unclear origin, possibly associated with the atmospheric aging of primary emissions.

In this study, we set out to expand the discoveries of ref. 27 in order to study in much greater depth the different sources of DMA and TMA. This includes analysis of: (a) precise analytical measurements of simultaneous ambient atmospheric alkylamines collected at Signy and Halley in 2019, by air mass analysis and remote sensing; (b) in situ water measurements of different types of alkylamines in coastal and open water as well as melting sea ice collected during the PI-ICE cruise (Polar atmosphere-ice-ocean Interactions: Impact on Climate and Ecology[24,28,29]), occurring within the same time period as the atmospheric samples taken at Signy and Halley[27], (c) a comparison with chemical composition of aerosol samples collected in the same region in previous studies[14,28,29] and (d) alkylamines gas-particle partitioning theoretical calculations.

To our knowledge, this is the first simultaneous multi station study reporting a detailed chemical source apportionment of specific tracers of secondary aerosol formation processes in the Southern Ocean. We infer that different eco-regions contribute to specific aerosol populations, hence we claim their overlooked climate relevant importance. We show that DMA and TMA do not share similar emission sources, and their abundances vary remarkably across different polar eco-regions.

Results and discussion

Alkylamine concentrations in atmospheric samples

Figure 1 shows 5-day air mass back trajectories arriving at Halley and Signy, while simultaneously PM_1 aerosol samples were collected at both sites over 42 days. The majority of the time during the 5 days prior sampling, those air masses had travelled over OO and SI regions. Here, we use 'sea ice' and 'sympagic' interchangeably for ice-containing regions, and 'pelagic' and 'open ocean' interchangeably for ice-free regions. Figure 1 shows the large extent of the air masses studied given the achievement of simultaneous sampling at two stations located apart from each other and characterized by different air mass origin due to the Antarctic Circumpolar Current (ACC). Whilst the Signy samples were collected from air masses that had previously travelled almost entirely within the Boundary Layer (BL - 97 ± 10% of the time), a different scenario was seen at Halley, where only 59 ± 24% travelled within the BL. The local meteorological data did not present any clear difference between the two periods. Overall, average local meteorological conditions at Halley were temperature of −5 ± 1 °C, Relative Humidity (RH) 82 ± 3%, Wind direction (WD) 117 ± 60° and Wind speed (WS) of 2.5 ± 2 m/s. The Signy meteorological data showed overall warmer average temperature 0.3 ± 1 °C, and similar conditions (RH 89 ± 3%, WD of 248 ± 10° and WS 2.9 ± 3 m/s).

Supplementary Fig. S1 summarize the main chemical species as reported before[27]. Whilst similar concentrations of water soluble PM_1 in the simultaneous samples collected at the two stations were found (Signy and Halley, 0.87 ± 0.4 and 0.8 ± 0.6 μg m^{-3}) - Signy was mostly represented by primary sea salt (43%) whereas Halley mostly by secondary nss-SO_4^{2-} (59%). By contrast, similar concentrations of non-MSA WSOM (0.15 ± 0.07 and 0.13 ± 0.07 μg m^{-3}) were found[27]. Figure 2a shows that also similar MSA concentrations were found at the two monitoring sites (0.08 ± 0.04 and 0.06 ± 0.04 μg m^{-3}). This may be surprising given Halley is on the Brunt ice-shelf, hundreds of kilometres from major DMS sources. However, the observed enrichment of nss-SO_4^{2-} with respect to MSA for aged air masses with low DMS content at Halley is in line with other studies[30]. The data collected at Signy-Halley reported similar concentrations of MSA among the two sampling stations, although the MSA/nss-SO_4^{2-} ratio was found about twice as high at Signy relative to Halley (0.55 versus 0.24), suggesting latitude trends evidenced before[31].

In this study, we focus on alkylamine concentrations. We report Ion Chromatography measurements (IC) of selected alkylamines (mono-, di- and tri- methylamine – MMA, DMA, and TMA, respectively; ethylamine – EA; diethylamine – DEA). Specifically, Fig. 2b reports DMA and TMA concentrations, which were the major alkylamines detected in the study.

The concentration trends of DMA and TMA were not expected. Whilst similar concentrations were found for DMA at both sites (1.2 ± 0.08 and 1.4 ± 1.1 μg m^{-3}), a striking eighty-fold more TMA was found at Signy (7.8 ± 4.1 ng m^{-3}) relative to Halley (0.1 ± 0.1 ng m^{-3}). MMA was also found at ten-fold more at Signy (1.0 ± 0.7 ng m^{-3}) than at Halley (0.1 ± 0.05 ng m^{-3}). Our results suggest that MMA and TMA show the

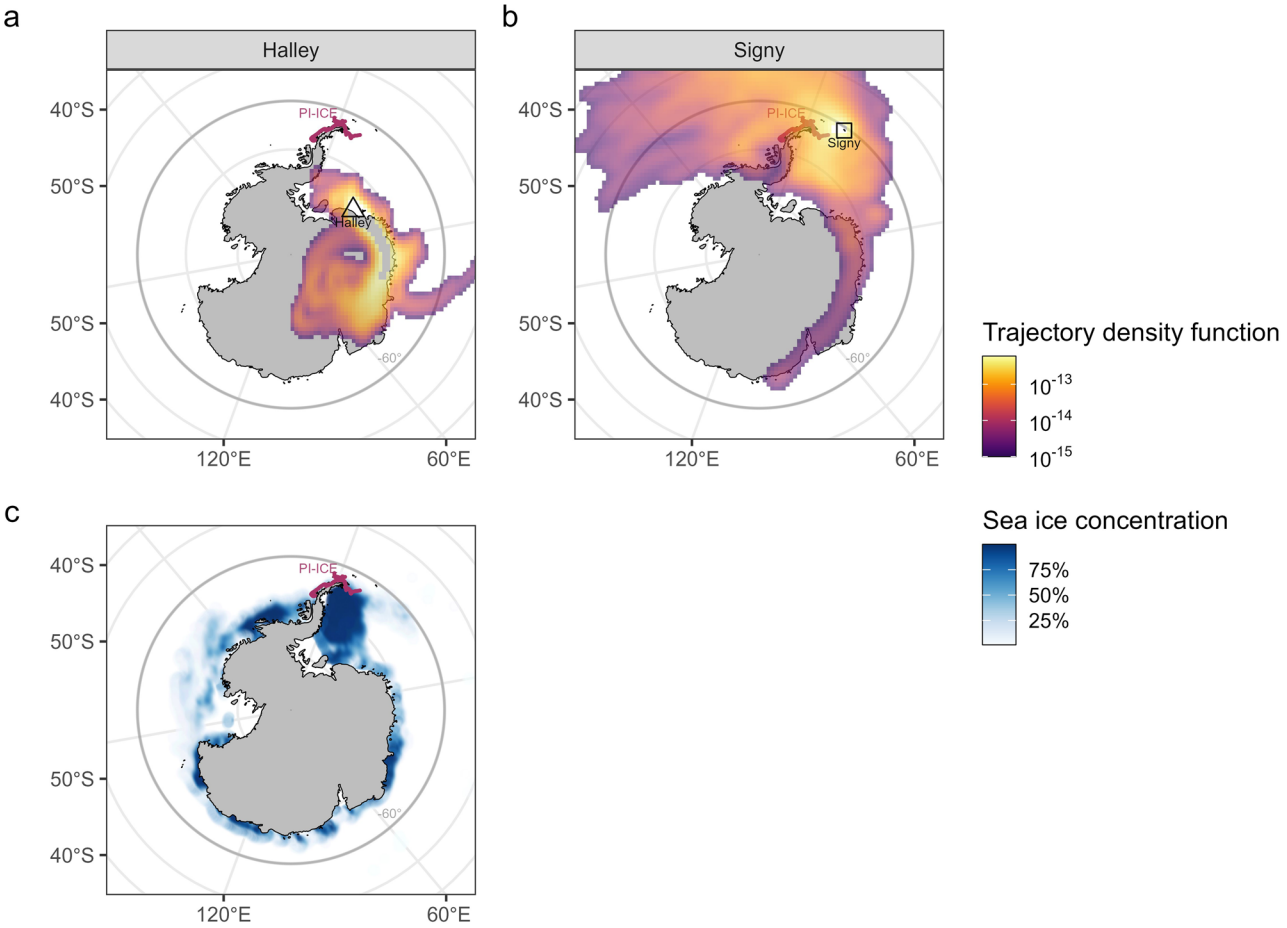

Fig. 1 | Apportioning of the origin of organic nitrogen in aerosols. Maps of the study area with BAS HAlley (triangle marker, **a**) and Signy (diamond marker, **b**) stations, and Sea ice concentration maps for the period of study (January–February 2019). Please note that air mass back trajectories for the all the sampling periods at both stations are plotted in **a** (Halley) and **b** (Signy) as trajectory density funcion. Sea ice maps (**c**) are plotted for the period of study (January–February 2019).

greater regional difference, and the two compounds may have the same origin, as discussed later in the manuscript. Other alkylamines (EA and DEA) were found in very low concentrations (EA 0.01 ± 0.01 ng m^{-3} and DEA, 0.23 ± 0.16 ng m^{-3}) at Halley, and were below LOD at Signy.

Our results for the first time show remarkable differences in the speciation of different alkylamines in different regions across the Southern Ocean and Antarctica. In other words, whilst we previously presented data showing more amines in the SI regions[14,21], here we show a remarkable alkylamines speciation in different Antarctic atmospheric regions. Our observation points to the existence of multiple amine sources and therefore aerosol formation processes in the different sympagic and pelagic studied areas.

Source apportionment overlaps with air mass back trajectory analysis and remote sensing

The individual measurements of DMA and TMA plotted in Supplementary Fig. S2 show a sharp variation in concentrations between samples. When we plotted air mass back trajectories for the strongest alkylamines signal detected in an ambient aerosol sample (S14), we find all air masses are travelling over extensive sympagic regions (Supplementary Fig. S3).

To specifically elucidate aerosol sources, we then ran a geographical source attribution study by calculating concentrated weighted trajectories (CWT) for our aerosol phase data. We grid back trajectories to 1 × 1 degree squares and weighed each segment of the back trajectory with the corresponding aerosol concentrations observed upon the air mass's arrival. The main components are plotted in Fig. 3. As expected, non-MSA Water Soluble Organic Matter WSOM (Fig. 3a) is mainly seen in the Southern Ocean pelagic open water. This is similar to the sea salt (Fig. 3b), likely associated with the organic component of the sea spray, also in line with previous research cruises[14]. The main secondary components seen in Fig. 3c, d (nss-SO_4^{2-} and MSA) are seen broadly over large Southern Ocean and Antarctic regions, reflecting the regional secondary component. When comparing DMA and TMA, Fig. 3d, e provides convincing visual evidence of markedly different sources in the study areas. Whilst DMA is mainly associated with OO regions characterized by pelagic waters, we find a hot spot of TMA associated with the sympagic region of the Weddell Sea. Our mapping analysis overlapped with precise analytical atmospheric measurements reveals extensive differences over different regions, supporting the initial findings showing that the microbiota of sea ice and sea ice-influenced (sympagic) ocean are a significant source of atmospheric organic nitrogen aerosols[14]. However, this study shows that TMA – and not all alkylamines – are related mainly to sea ice regions.

The sea ice extent in the Weddell Sea contains the largest percentage of Antarctic multiyear ice of any sector of the Southern Ocean[32], and during its maximum cover, it represents about 40% of the total Antarctic Sea ice cover. The marginal ice zone (MIZ) in the Antarctic is the largest in the world ocean[33]. There is a growing body of observations posing a problem of having a proper description of the Antarctic MIZ and of Antarctic sea ice variability in general because of (a) mixed types of sea ice, (b) waves penetrating deep into pack ice and (c) drifting of sea ice in correspondence of large-scale synoptic events[33–36]. This vast biome composed of multiple habitats is an

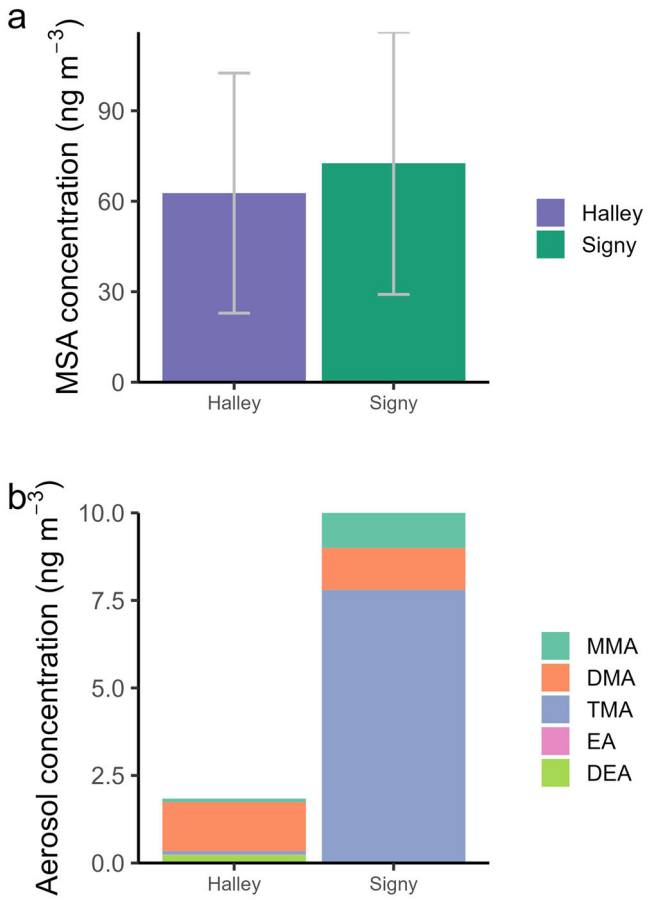

Fig. 2 | Average concentrations at Signy and Halley for the overlap period of 42 days. a Average concentrations for MSA and **b** average concentrations for the 5 alkylamines measured (MMA, DMA, TMA, EA, DEA).

important component of the Earth's climate system but a spatially complex physical environment with melt ponds, ice floes and surrounding sea water. In a further analysis, we calculated how far each air mass travelled over zones distinguished by their surface characteristics. We define the following regions: (a) Southern Ocean Pelagic waters (regions of open water situated at latitudes lower than 60° South, "SOP"), (b) Antarctic Sympagic waters (regions with sea ice concentrations lower than 15% situated at latitudes higher than 60° South, "AS"), (c) Marginal sea ice zone (regions with sea ice concentration higher than 15% and lower than 80% within the consolidated ice region, "MIZ"), (d) Dense sea ice regions (regions with pack ice concentration higher than 80%, in other words regions with dense sea ice concentrations, between 80% and 100%, ice fracturing and opening of leads, small areas of open water surrounded by sea ice floes) and (e) Total sympagic regions (>60°S open water and sea ice regions, "TS", the sum of b–d).

Whilst MSA and total alkylamines do not provide any clear trends, the Pearson correlation coefficient values reported in Table 1 give a mathematical expression of the visual results appreciated in Fig. 3e, f.

First, there is an opposite trend between DMA and TMA concentrations versus Pelagic SOP waters: the former correlating ($r = 0.49$) and the latter anticorrelating ($r = -0.59$). Second, there is an opposite correlation between DMA and TMA concentrations versus Dense sea ice regions (mainly represented by the Weddell Sea region): the former anticorrelating ($r = -0.45$) and the latter correlating ($r = 0.63$). Third, there is a clear anticorrelation between DMA concentrations and regions of Marginal Sea ice zone MIZ regions ($r = -0.45$), Total sympagic regions ($r = -0.73$) and Antarctic Sympagic waters ($r = -0.55$). The overall results of Table 1 strongly confirm that DMA may be related mainly with pelagic regions whereas TMA is mainly associated with sympagic regions, specifically to the dense sea ice Weddell Sea region (positive correlation (d) of $r = 0.63$ shown in Table 1).

Correlation between alkylamines and MSA

We wanted to study the expected correlation between secondary organic aerosol species including Alkylamines and MSA. However, when we plotted the DMA versus the TMA, we could not really find any correlation among DMA, TMA and MSA (Supplementary Fig. S4) when both monitoring sites are considered. Our results imply a complex relationship among the three secondary species, that one would expect to correlate with one another. We therefore ran a Principal Component Analysis (PCA, see methods) to further understand the absence of the expected correlation between MSA and Alkylamines shown in Supplementary Fig. S4. We took a large dataset (see Supplementary Fig. S5) – a total number of 45 aerosol samples from previous studies (7 from PEGASO[14], 22 from Signy-Halley[27], and 16 from bubble bursting experiments (PI-ICE)[28,29]). We considered nine variables from the speciation provided by the H-NMR spectroscopy in protic solvents described elsewhere (see methods): WSOC, aliphatic chains, polysubstituted aliphatic chains, aliphatic hydroxyl/alkoxy groups, anomeric and vinylic groups, aromatic functionalities, MSA, DMA and TMA. Results of the nine variable PCA loadings are seen in Supplementary Fig. S6, and the relative PCA plots in Supplementary Fig. S7a–f.

One PCA component (PC1) is associated mainly with the primary sea spray organic component, explaining about 67% of the variance (PC1, Supplementary Fig. S6), as seen in the red B dots in Supplementary Fig. S7a–f.

Samples from Signy S4 and Signy S5 are on the top right side of the diagram because they are unique in the very high amount of WSOC due to the stormy conditions (as reflected also in the highest sea spray concentrations of the entire field study[27]). By stark contrast, two different types of PC components associated with secondary components can be seen. PC2 (about 21%) is associated with MSA and DMA, whereas PC3 (about 11%) is mainly associated with MSA and TMA (Supplementary Fig. S6). When PC2 is plotted versus PC3 (Supplementary Fig. S7c), we clearly see two different groups describing three different datasets collected in the Antarctic region[14,27–29]. First, the positive values of PC3 and positive ones of PC2 (top right part of the diagram) have the samples of S6–S14 of Signy, with major contributions from sample S11 and S14, the two strongest TMA components (see also Supplementary Fig. S2). By contrast, the negative values of PC3 and positive values of PC2 (bottom right part of the diagram) are mainly described by samples collected at Halley. Specifically, mostly with sample H7 and H8 due to long range aged air masses from OO regions. Our analysis suggests that different types of alkylamines may be associated with local boundary layer and free-tropospheric circulations. Remarkably, the aerosol data previously presented from the PEGASO cruise[14,23] fit the interpretation. The three samples on the right panel of Supplementary Fig. S7c are PEG 0901, PEG 1301 and PEG 1801, which are the three samples mainly associated with sympagic air masses. The uniqueness of PEGASO A1801 relies in being the only one out of the eight PEGASO sample mainly associated with Weddell air masses[23] presenting the highest concentrations of Alkylamines found during the cruise[23]; air masses are summarized in Supplementary Fig. S8.

Gas phase and aerosol calculations

Given the TMA concentrations observed in aerosol samples and applying the gas-particle partitioning equation by ref. 37, based on a pH dependent formulation of the effective Henry's law Constant (K_H), it is possible to estimate the corresponding theoretical gas-phase concentrations of the alkylamines at the equilibrium. Aerosol liquid water content (LWC) and pH were calculated by the ISORROPIA-II model[38–42] using the chemical composition of ambient aerosol and meteorological data already described in ref. 27 (see also Supplementary Table S1). Aerosol LWC and pH resulted in average values of 2.32 μg m^{-3} and 1.82, respectively in the Weddell Sea impacted samples collected at Signy. Under such conditions, only 17% of TMA on average is expected to partition to the particle phase, meaning that

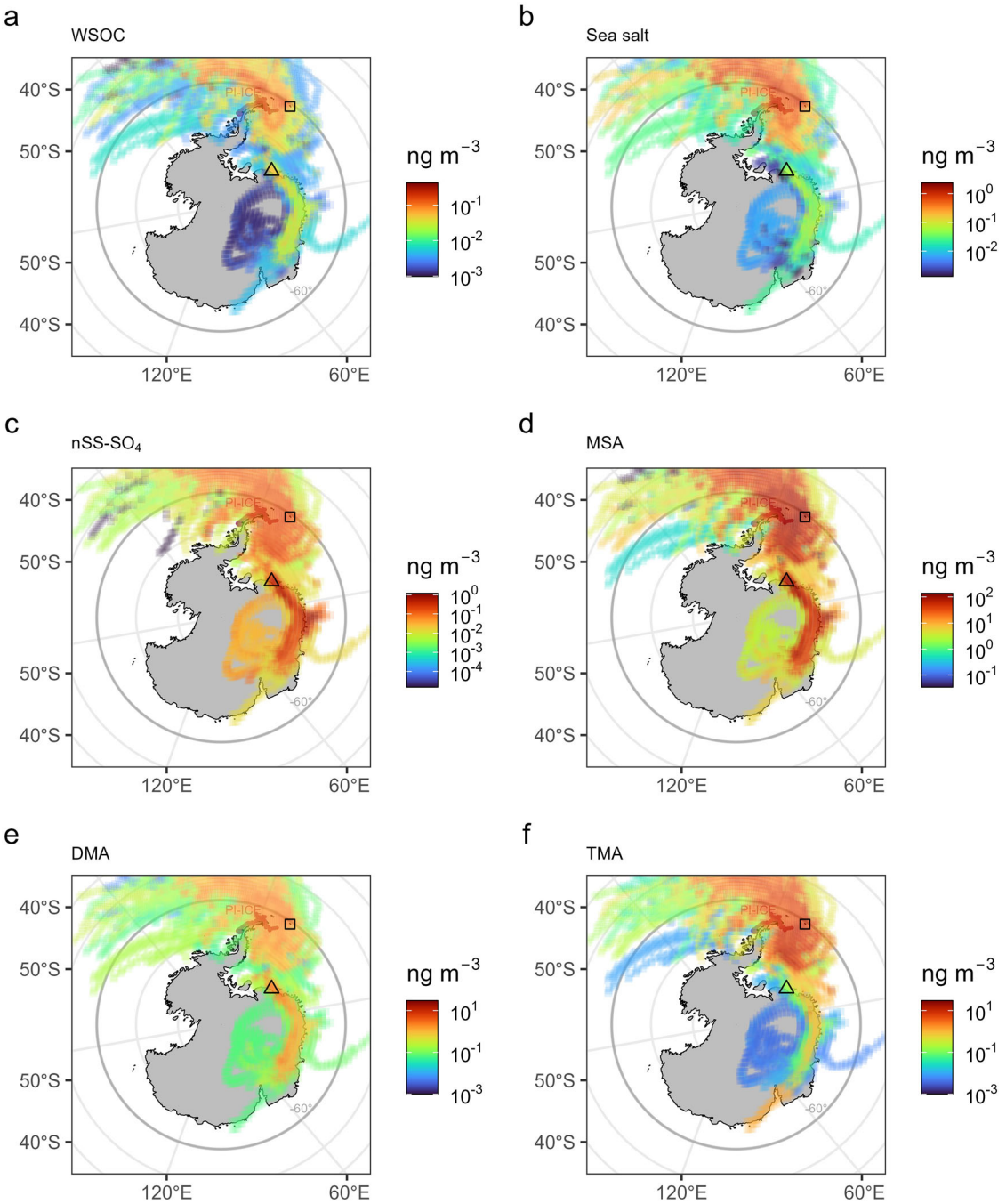

Fig. 3 | CWT maps of the chemical components identified at Signy and Halley. Specifically, maps are shown for **a** non MSA WSOC, **b** Sea salt, **c** nss-SO, **d** MSA, **e** DMA and **f** TMA. The colour scale shows which air masses along the back trajectories have, on average, higher concentrations at the measurement site: lighter colours (toward yellow) and darker colours (toward blue) indicate respective higher and lower concentrations of the component associated with the air masses coming from a specific area.

83% of total TMA would remain in the gas-phase. This implies that the strength of the Weddell Sea as a source of TMA is even higher than what aerosol samples alone would suggest. Given the average concentration of TMA of 7.8 ng m^{-3} determined in the PM_1 samples at Signy, it can be estimated a potential concentration of gaseous TMA of the order of 38 ng m^{-3} (~14 ppt) over the area of the Weddell Sea during our study.

Measurements of alkylamines in water and melting sea ice samples

Reference 21 reported that concentrations of mono-, di- and trimethylamine (MMA, DMA and TMA, respectively), and their precursors, the quarternary amines glycine betaine and choline and simple aminoacids (glycine), were enhanced in sympagic sea water samples relative to ice-devoid pelagic ones. In this study, simultaneously with the measurements at Signy and Halley, a number of shipbase measurements took place aboard the RV Hesperides between 25 January 2019 and 4 February 2019 around the South Shetland Islands (around 63° S), sailing down to 68° S over several days to Adelaide Island, and then back to the South Shetland Islands during the PI-ICE cruise (see Supplementary Fig. S5). Whilst we were not able to collect atmospheric shipborne measurements of alkylamines due to an instrument failure of the sampling system, we succeeded in sampling

Table 1 | Correlation plot table (r) for selected chemical species (TMA, DMA, TMA + DMA, MSA) with different surface types where air masses had previously travelled (120 h total time)

	Selected chemical compounds (Aerosol PM_1)			
Air mass travel surface type	**DMA**	**TMA**	**Total Alkylamine (TMA + DMA)**	**MSA**
(a) Southern Ocean Pelagic waters (regions of open water situated at latitudes lower than 60° South, "SOP")	0.49	−0.59	–	–
(b) Antarctic Sympagic waters (>60°South)	−0.55	–	–	–
(c) Sympagic less dense sea ice zone (Marginal sea ice zone, MIZ, 15%-85% ice)	−0.45	–	–	–
(d) Sympagic more dense sea ice zone (sea ice >85–100%), mainly the Weddell sea area)	−0.45	0.63	–	–
(b + c + d) Total sympagic areas (>60°S water and sea ice regions)	−0.73	–	–	–

Only r higher than 0.45 are shown in the table.

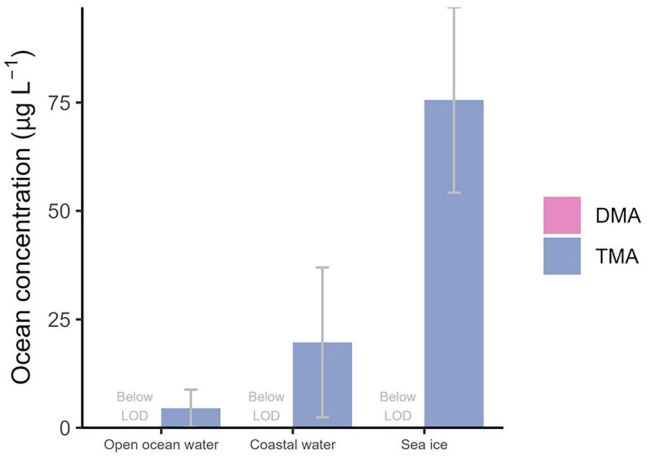

Fig. 4 | Water concentration of DMA and TMA for open ocean water ($N = 5$), coastal water ($N = 7$) and melting sea ice samples ($N = 3$). DMA was always below detection limit in this study.

and detecting alkylamines dissolved into coastal and open ocean seawater as well as from melting sea ice samples (see methods). Results are shown in Fig. 4, highlighting the highest average concentration in sea ice samples, once again confirming the sea ice as a source of organic nitrogen, and specifically of TMA. We also see a gradient in coastal waters, this can be due to melting of coastal land-sea ice floes, but also to other media including Antarctic seaweeds (benthonic macroalgae[28,43,44], seabird populations[28,29,45,46] and other unknown terrestrial sources. Our results suggest the presence of coastal hotspots additional to the regional oceanic open ocean and sea ice sources of alkylamines. The concentrations of TMA measured in this study were 4.3 ± 4.3 nM and 19.7 ± 17.3 nM for open ocean and coastal seawater samples, respectively: higher than those previously reported for seawater, but within the same order of magnitude[47]. The sea ice concentrations were instead 3–4 times higher than the seawater samples (i.e., 75 ± 21.4 nM). Studies of methyl-amines (MAs) in the Antarctic region reported concentrations from 0 to 5.9 nM in Marguerite Bay, Antarctica[48], through to 0 to 2.9 nM off the North Orkney Islands, in the Southern Ocean[14], where MMA and TMA, respectively, were the most abundant MAs. Although the relative analyte abundance was lower in previous studies, the reduction in concentration with distance from land is consistent with the trend observed for the present study. During this study, DMA and MMA concentrations in all water samples were below detection limit. However, by using a novel method, DMA has been detected in other recent samples from productive, coastal Antarctic waters[49]; suggesting our DMA measurements are likely systematically undermeasured in the total alkylamine concentrations in the sampled water. The observed methylamines were aligned neither with physical parameters nor with phytoplankton biomass or chlorophyll a, and nanoflagellates were possibly attributed as main source.

Atmospheric implications

Aliphatic amines are known to be important ingredients for aerosol formation in the marine atmosphere[18,22,24], but their sources are not well apportioned. In the ocean, alkylamine in aerosol particles may derive from secondary gas to particle conversion as well as primary mechanisms from surface waters to the atmosphere by bubble bursting. This first simultaneous detection of alkylamines in the atmospheric aerosol at two Antarctic sites enables the reporting of unique insights into their temporal patterns and abundance variations. Our study strongly supports previous studies demonstrating that the microbiota of sea ice and the sympagic ocean is a source of low molecular weight alkylamines, likely shifting from sea water to atmospheric secondary aerosols due to the low pH expected in fine particles[14,20,21].

The knowledge of alkylamines in the Oceans is very limited, some precursors include glycine betaine (GBT) and trimethylamine N-oxide (TMAO)[48,50,51]. These are made by a number of ecosystems to counteract fluctuations in salinity[52]. GBT is biologically degraded first generating TMA, following further degradation to DMA and MMA[52–54]. Our results are in line with such studies because we find the highest amount of alkylamines in the most severe salinity gradients: marine organisms in the sea ice and sympagic regions need to maintain osmotic pressure under different salinity conditions. Finally, the scarcity of measurements does not allow us to discuss the relative role of marine and terrestrial sources of alkylamines in Antarctica, although ref. 20 showed no major relation with seabird emissions. It remains a very open question as to the relative apportionment of alkylamines from local (i.e. guano[46,55] or other materials) versus regional (i.e. sea ice regions) sources in the Antarctic atmosphere. In our previous work in the study areas[27], we reported five organic aerosol (OA) sources: two primary organic aerosol (POA) types linked with open-ocean and sympagic/coastal waters, respectively; two secondary organic aerosol (SOA) types, also linked with open-ocean and sympagic/coastal waters, respectively; and a fifth component of unclear origin, possibly associated with the atmospheric aging of primary emissions. The analysis did not reveal any major input of local sources, but further studies are needed to apportion the total budget of organic nitrogen in the Antarctic bioregions.

Uncertainties remain also in the chemical reactivity of autoxidation products in both gas and aqueous phase, as well as their phase partitioning[56].

Here, we attempt to compare our unique Antarctic dataset with marine datasets collected in other Oceans. It is imperative to remember that - even in the Southern Ocean - it is clear that sympagic and pelagic areas are different, as seen in this study and elsewhere[57]. Furthermore, for example, ref. 17 identified three main aerosol sources in the SO: the Northern (40–45 S), Mid-latitude (45–65 S) and Southern sectors (65–70 S), with different mixtures of continental and anthropogenic, primary and secondary aerosols depending on the studied region. During the same period of study, ref. 58

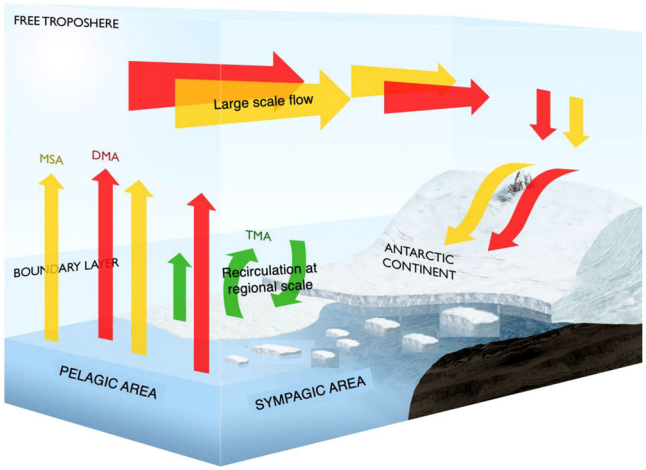

Fig. 5 | Graphical abstract of the measurements described in this study. We take expand the conceptual diagram from Lachlan-Cope et al. (2020), where we presented a schematic illustration of the ultrafine new particle formation (NPF) and new particle growth (NPG) aerosols in Antarctica.

found a weak gradient in CCN at 0.3% supersaturation with increasing CCN concentrations to the south between 44 and 62.1 °S, which may be caused by aerosol precursors from Antarctic coastal biological emissions. Again, comparing the North Southern Ocean (NSO) (50°S–60°S) and the South Southern Ocean (SSO) (62°S–68°S), ref. 59 reported a very different aerosol hygroscopicity growth factor of 1.41 for aerosols with 50 nm < D < 250 nm over the SSO, but increased from 1.30 to 1.67 over the NSO, indicating striking distinct chemical compositions over the Southern Ocean. Our study supports the growing evidence of different aerosol regions across the Southern Hemisphere.

A large body of literature on ocean-atmosphere alkylamine measurements associated with marine areas is derived from measurements near China. Reference [60] proposes how the largely increased primary TMA and secondary DMA are linked to emissions of sea-spray aerosols and gaseous precursors from various cyclonic eddies. Recent laboratory and ambient measurements provide evidence that particulate marine alkyl aminium ions may not only originate from the gas-to-particle conversion of the gaseous precursors but also can be the products of the degradation of larger N-containing species in the aqueous phase[53,54,61]. During a cruise campaign over the Chinese marginal sea, a significant correlation between the four aminiums (Monomethylaminium MMAH, dimethylaminium DMAH, ethylaminium EAH and diethylaminium DEAH, protonated forms of MMA, DMA, EA and DEA) and methanesulfonic acid suggested their secondary formation pathways; whereas trimethylaminium (TMAH, the protonated form of TMA) showed moderate correlation with sodium, suggesting its primary marine sources via enrichment in the sea-spray aerosol through bubble bursting[62].

Our data, instead, suggest a marine source of DMA, in particular associated with pelagic Southern Ocean, while TMA is clearly linked with the sympagic environment (Fig. 5). Furthermore, considering aerosol alkyl-amine formation processes, all the collected evidence suggests that – over Antarctica – secondary formation routes are dominant both for DMA and TMA, as already addressed[14,21]. Our Antarctic data also diverge from a recent emission inventory based on multi-source data sets estimating the contribution of marine biological emissions to gaseous methylamines in the atmosphere showing that the Oceans can act as a sink for DMA and source for TMA while it can be either a source or sink for MMA[63,64].

We argue that – contrary to the other Oceans – our pelagic and sympagic Southern Ocean data shows that (1) the ocean is a source of both DMA and TMA, the former mainly associated with pelagic regions and the latter mainly with sympagic regions; and (2) not only DMA, but also TMA is mostly secondary according to our data, given the TMA/SSA ratios are much higher in ambient samples relative to bubble bursting primary aerosols (pointing mainly to secondary routes).

Atmospheric alkylamine concentrations are globally much lower than ammonia[65]; however, we have already demonstrated that local emissions can increase their concentrations in specific regions (such as the Weddell Sea area). Moreover, ppt concentrations of dimethylamine[66] (DMA) and trimethylamine[67] (TMA) can enhance the nucleation of sulphuric acid by orders of magnitude relative to ammonia[6,67]. DMA can also form stable clusters with iodine oxoacids, and the enhancement to NPF rates will be greatest in environments like Antarctica where iodine precursor concentrations are low[68]. Small fluxes of DMA and TMA to the gas phase can therefore enhance the rate at which gases transform into ~1.5 nm particles. Measurements in the Antarctic peninsula have shown DMA[18], MMA, TMA, and DEA clustered with sulphuric acid, indicating a key role in particle formation. Gas-phase amines have a lifetime of hours with respect to oxidation by OH[69], and therefore any enhancement to NPF will be relatively localised to the sources. We show, consistent with previous studies, that the sympagic regions of Antarctica are a source of alkylamines, and therefore suggest that NPF will be enhanced in a range of tens to hundreds of kilometres surrounding sympagic regions of Antarctica.

In summary, we shed some light into the complexity of aerosol processes in different Antarctic bioregions. Southern Ocean and Antarctic bioregions possess strong environmental gradients. The changing Antarctic environment will feed back to climate via exchanges between the biosphere and the cryosphere with the atmosphere. Our interdisciplinary study using both ocean and atmospheric data with remote sensing statistical analysis helps to tease out processes across spatial gradients where different ecosystems regulating the atmospheric concentrations of aerosols.

Methods

Measurements air sampling

The measurements reported here were made in the framework of PI-ICE (Polar Interactions: Impact on the Climate and Ecology) study in the period December 2018–March 2019 at the British Antarctic Survey's stations of Halley and Signy. BAS Halley VI station (75°36'0" S, 26°11'0" W) is located in coastal Antarctica, on the floating Brunt Ice Shelf about 20 km from the coast of the Weddell Sea. A variety of measurements were made from the Clean Air Sector Laboratory (CASLab), which is located about 1 km south-east of the station[70]. BAS Signy station at Signy Island (60°43'0" S, 45°38'0" W) is located in the South Orkney Islands (Maritime Antarctic) and is characterized by a cold oceanic climate, with mean annual air temperature of 3.5 °C and annual precipitation ranging from 350 to 700 mm, primarily as summer rain.

Two high volume samplers (MCV Barcelona Spain, equipped with Digitel PM_1 sampling inlet) at Signy and Halley collected ambient aerosol particles with particle diameter (Dp) < 1 µm on pre-washed and pre-baked quartz fibre filters, at a controlled flow of 500 L min^{-1}. Due to the necessity of collecting sufficient amounts of samples for detailed chemical analyses, sampling time was of the order of about 50 h for each sample. A total of 8 and 14 PM_1 samples were collected during the field study at Halley and Signy stations, respectively. The samples were stored at about −20 °C until extraction and chemical analyses.

Air mass back trajectories analysis and source regions classification

Five day back trajectories arriving at a height of 30 m every 6 h were calculated using HYSPLIT - (Hybrid Single-Particle Lagrangian Integrated Trajectory v4)[71] and monthly Global NOAA-NCEP/NCAR pressure level reanalysis data archives. Using these, trajectory level plots were also calculated using the Openair package[72] using the Concentration Weighted Trajectory (CWT) method.

Aerosol offline measurements

The ambient PM_1 aerosol samples collected on quartz-fibre filters from both PEGASO cruise and the two sites of the PI-ICE campaign (i.e., Signy &

Halley) were extracted with deionized ultrapure water (Milli-Q) in a mechanical shaker for 1 h and the water extracts were filtered on PTFE membranes (pore size: 0.45 μm) in order to remove suspended materials. Extracts were analysed by ion chromatography (IC) for the quantification of water-soluble inorganic ions (sodium, Na^+; chloride, Cl^-; nitrate, NO_3^-; sulfate, SO_4^{2-}; ammonium, NH_4^+; potassium, K^+; magnesium, Mg^{2+}; calcium, Ca^{2+}), organic acids (acetate, ace; formate, for; methanesulfonate, MSA; oxalate, oxa)[73] and low molecular weight alkyl-amines (methyl-, ethyl-, dimethyl-, diethyl- and trimethyl-amine, MA, EA, DMA, DEA and TMA, respectively)[74]. An IonPac CS16 3 × 250 mm Dionex separation column with gradient MSA elution and an IonPac AS11 2 × 250 mm Dionex separation column with gradient KOH elution were deployed for cations and anions, respectively. For more info, please refer to ref. 27. The complete dataset is also available at Zenodo Data public repository (https://doi.org/10.5281/zenodo.10663787). The sea-salt and non-sea-salt fractions of the main aerosol components measured by ion chromatography were derived based on the global average sea-salt composition found in ref. 75 using Na+ as the sea-salt tracer.

Principal Component Analysis (PCA) on aerosol offline data from PI-ICE and PEGASO expeditions

Principal Component Analysis (PCA) was applied to the larger dataset including aerosol samples also from previous works in the same study area. Specifically, in total 45 samples were used: 7 ambient PM1 samples from PEGASO[14,23]; 22 ambient PM_1 from Signy-Halley[27]; and 16 Sea-Spray Aerosol PM_1 samples from bubble bursting experiments conducted during PI-ICE[28,29]. Ship measurements took place between 25 January 2019 and 4 February 2019 aboard the RV Hesperides. For this statistical analysis we used the water-soluble organic carbon characterization and in particular the functional groups distribution provided by the H-NMR spectroscopy, as already described in refs. 23,27. Briefly, the 1H-NMR spectroscopy in protic solvents provides speciation of hydrogen atoms bound to carbon atoms and on the basis of the range of frequency shifts, the signals in the 1H-NMR spectra can be attributed to specific functional groups containing H–C bounds[76,77]. Organic hydrogen concentrations directly measured by 1H-NMR were converted to organic carbon using stoichiometric ratios specifically assigned to functional groups using the same rationale described in previous works[27,76,78].

Moreover, specific organic molecules can be univocally identified in the 1H-NMR spectra on the basis of their characteristic patterns of resonance and chemical shifts. Among the tracers identified in the PEGASO and PI-ICE samples, MSA and two low-molecular-weight alkyl-amines (di- and trimethyl amines, DMA and TMA respectively) were quantified in mass concentrations and validated against the IC measurements[27]. In conclusion, in the application of PCA we considered nine variables: the mass concentrations of WSOC (as measured by TOC-analyzer - Shimadzu TOC-5000A), 5 functional groups (namely, aliphatic chains, polysubstituted aliphatic chains, aliphatic hydroxyl/alkoxy groups, anomeric and vinylic groups, aromatic functionalities), and 3 organic tracers (i.e., MSA, DMA and TMA), as quantified by H-NMR.

Thermodynamic analysis and estimations of aerosol LWC and pH

We applied on the PM_1 samples from Signy and Halley stations the ISORROPIA-II (version 2.3) aerosol thermodynamic model[38] (http://isorropia.epfl.ch), which calculates the composition and phase state of a K^+–Ca^{2+}–Mg^{2+}–NH_4^+–Na^+–SO_4^{2-}–NO_3^-–Cl^-–water inorganic aerosol in thermodynamic equilibrium with gas-phase precursors. ISORROPIA-II has been extensively used to predict the liquid water content and pH for inorganic aerosol[39–42,79,80]. Similar to previous studies, the pH is calculated here according to the following equation:

where γ_{H+} is the hydronium ion activity coefficient (here assumed unity), H_{aq}^+ (mol L^{-1}) is the hydronium ion concentration in the aerosol aqueous phase, H_{air}^+ (μg m^{-3}) is the hydronium ion concentration per volume of air, and W_i and W_o (μg m^{-3}) are particle water concentrations associated with the aerosol inorganic and organic species, respectively.

The pH used here is consistent with the pH_F definition of ref. 81. In this work, we neglect the contribution of water from organic species and their overall effect on water activity and pH. References 39,82–84 evaluated this assumption and found organics to have a secondary effect on aerosol pH, somewhere between 0.15 and 0.3 pH units. So, since the organic aerosol hygroscopicity is not measured in our study and given that neglecting Wo appears to have only a minor impact on the pH characterization, we determine pH only considering Wi.

We used ISORROPIA-II in the partitioning ("forward") mode for metastable aerosol. In this configuration, the model calculates the equilibrium partitioning given the total concentration (gas plus particles) of various species together with RH and T as input. Here we apply the partitioning mode using just the ionic composition of PM1 samples considering gaseous ammonia and nitric acid concentrations negligible in such a marine remote environment of the study area (i.e., Antarctica stations of Signy and Halley).

Water measurements and sample collection and analysis

Ship measurements took place between 25 January 2019 and 4 February 2019 aboard the RV Hesperides[28,29] near the Antarctic peninsula. Seawater volumes of 1 L were obtained using CTD or underway sampling procedures. Samples were collected and filtered through 0.7 μm glass fibre filters (GF/F). Filtered water was immediately acidified at a ratio of 1:1000 v/v (acid : solution). Once preserved, filtered samples were stored in a fridge at 4 °C for the duration of the research cruise. Samples were transported to Plymouth under chilled conditions and stored at 4 °C prior to analysis.

Samples were prepared for solid phase microextraction (SPME) along with blanks and calibration standards for MAs. Standards and samples were pipetted into glass vials with screw caps that were compatible with the RSH Triplus autosampler. Sample aliquots (10 mL) were pipetted into 20 mL glass vials and saturated with NaCl to achieve 33% salt content (w/v). And internal standard (cyclopropylamine) was added to each vial to a final concentration of 8.7 nM. The pH of the solution was adjusted to >13.0 by adding 10 M NaOH solution (250 μL) and the vials immediately sealed. Blank samples comprised high purity water (18.2 MΩ cm resistivity) treated with NaCl and NaOH as described. Stock and working standard solutions were prepared regularly.

The amines were extracted from samples using a TriPlus RSH autosampler system (Thermo Fisher Scientific) with an integrated SPME procedure. Analytes were extracted onto an SPME fibre after equilibration in an integrated oven, followed by injection and exposure of the SPME fibre coated with Polydimethylsiloxane/Divinylbenzene (65 μm × 10 mm; Merck, UK). The fibre was then exposed in the injector of the gas chromatograph (GC), containing a base-deactivated liner, where the analytes were thermally desorbed and transported onto the GC column.

$$pH = -\log_{10}\gamma_H + H_{aq}^+ = -\log_{10}\frac{1000\gamma_H + H_{air}^+}{W_i + W_0} \cong -\log_{10}\frac{1000\gamma_H + H_{air}^+}{W_i} \quad (1)$$

The separation and detection of MAs were performed on a Thermo Scientific Trace 1300 Series Gas Chromatograph (Thermo Fisher Scientific, UK). Analytes were resolved on a 0.32 mm (i.d.) × 60 m CP-Volamine column and measured on a nitrogen-phosphorus detector equipped with a rubidium bead. Detector gases (nitrogen, hydrogen, and zero air) were supplied through Precision Series GC gas generators (Peak Scientific, UK), specifically, a Nitrogen 250-GC N_2 generator, a Hydrogen 200 H_2 generator, and a Zero air 1.5 gas generator. Helium (N5.0 grade, BOC, UK) was used as the carrier gas (flow rate 1.38 mL min^{-1}). The flow rate of the detector gases H_2 and air was 60 and 3.5 mL min^{-1}, respectively, while the nitrogen make-up gas had a flow rate of 15 mL min^{-1}. The injector and detector temperatures were 250 and 300 °C, respectively. The initial oven temperature was 40 °C (2 min), which increased to 130 °C at a rate of 10 °C min^{-1}, then to 260 °C at a rate of 50 °C min^{-1}, where it was held for 4.4 min. Data

acquisition and processing that yielded peak areas was performed by Thermochromeleon vs. 7.3 software[85]. All samples were analysed in triplicate ($n = 3$).

Data availability

The aerosol composition dataset is publicly available at Zenodo Data public repository (https://doi.org/10.5281/zenodo.10663787). The rest of the data will be deposited openly in a depository. Additional requests for materials, including from Supplementary Materials, should be addressed to M.D.O.

Received: 6 May 2025; Accepted: 25 November 2025;
Published online: 12 December 2025

References

1. IPCC. Summary for policymakers. In *Climate Change and Land: An IPCC Special Report on Climate Change, Desertification, Land Degradation, Sustainable Land Management, Food Security, and Greenhouse Gas Fluxes in Terrestrial Ecosystems* (ed. Shukla, P.R.) (IPCC, 2019).
2. Bodas-Salcedo, A., Williams, K., Field, P. & Lock, A. The surface downwelling solar radiation surplus over the southern ocean in the met office model: the role of midlatitude cyclone clouds. *J. Clim.* **25**, 7467–7486 (2012).
3. Carslaw, K. S. et al. Large contribution of natural aerosols to uncertainty in indirect forcing. *Nature* **503**, 67 (2013).
4. Hamilton, D. Natural aerosols and climate: Understanding the unpolluted atmosphere to better understand the impacts of pollution. *Weather* **70**, 264–268 (2015).
5. Schmale, J. et al. Overview of the Antarctic circumnavigation expedition: study of preindustrial-like aerosols and their climate effects (ACE-SPACE). *Bull. Am. Meteor. Soc.* **100**, 2260–2283 (2019).
6. Kirkby, J. et al. Atmospheric new particle formation from the CERN CLOUD experiment. *Nat. Geosci.* **16**, 948 (2023).
7. Kanawade, V. & Jokinen, T. Atmospheric amines are a crucial yet missing link in Earth's climate via airborne aerosol production. *Commun. Earth Environ.* **6**, https://doi.org/10.1038/s43247-025-02063-0 (2025).
8. Laskin, A., Laskin, J. & Nizkorodov, S. Chemistry of atmospheric brown carbon. *Chem. Rev.* **115**, 4335–4382 (2015).
9. Li, Y. et al. Nitrogen dominates global atmospheric organic aerosol absorption. *Science* **387**, 989–995 (2025).
10. SHAW, G. Considerations on the origin and properties of the Antarctic aerosol. *Rev. Geophys.* **17**, 1983–1998 (1979).
11. Brean, J. et al. Multiple eco-regions contribute to the seasonal cycle of Antarctic aerosol size distributions. *Atmos. Chem. Phys.* **25**, 1145–1162 (2025).
12. Charlson, R. J., Lovelock, J. E., Andreae, M. O. & Warren, S. G. Oceanic phytoplankton, atmospheric sulphur, cloud albedo and climate. *Nature* **326**, 655–661 (1987).
13. Quinn, P. K. & Bates, T. S. The case against climate regulation via oceanic phytoplankton sulphur emissions. *Nature* **480**, 51–56 (2011).
14. Dall'Osto, M. et al. Antarctic sea ice region as a source of biogenic organic nitrogen in aerosols. *Sci. Rep.* **7**, https://doi.org/10.1038/s41598-017-06188-x (2017).
15. Jung, J. et al. Characteristics of methanesulfonic acid, non-sea-salt sulfate and organic carbon aerosols over the Amundsen Sea, Antarctica. *Atmos. Chem. Phys.* **20**, 5405–5424 (2020).
16. Saliba, G. et al. Organic composition of three different size ranges of aerosol particles over the Southern Ocean. *Aerosol Sci. Technol.* **55**, 268–288 (2020).
17. Humphries, R. et al. Southern Ocean latitudinal gradients of cloud condensation nuclei. *Atmos. Chem. Phys.* **21**, 12757–12782 (2021).
18. Quéléver, L. et al. Investigation of new particle formation mechanisms and aerosol processes at Marambio Station, Antarctic Peninsula. *Atmos. Chem. Phys.* **22**, 8417–8437 (2022).
19. Lachlan-Cope, T. et al. On the annual variability of Antarctic aerosol size distributions at Halley Research Station. *Atmos. Chem. Phys.* **20**, 4461–4476 (2020).
20. Rinaldi, M. et al. Contribution of Water-Soluble Organic Matter from Multiple Marine Geographic Eco-Regions to Aerosols around Antarctica. *Environ. Sci. Technol.* **54**, 7807–7817 (2020).
21. Dall'Osto, M. et al. Simultaneous Detection of Alkylamines in the Surface Ocean and Atmosphere of the Antarctic Sympagic Environment. *ACS Earth Space Chem.* **3**, 854 (2019).
22. Dall'Osto, M. et al. Nitrogenated and aliphatic organic vapors as possible drivers for marine secondary organic aerosol growth. *J. Geophys. Res. Atmos.* **117**, https://doi.org/10.1029/2012JD017522 (2012).
23. Decesari, S. et al. Shipborne measurements of Antarctic submicron organic aerosols: an NMR perspective linking multiple sources and bioregions. *Atmos. Chem. Phys.* **20**, 4193–4207 (2020).
24. Brean, J. et al. Open ocean and coastal new particle formation from sulfuric acid and amines around the Antarctic Peninsula. *Nat. Geosci.* **14**, 383 (2021).
25. Kyrö, E. et al. Antarctic new particle formation from continental biogenic precursors. *Atmos. Chem. P hysics* **13**, 3527–3546 (2013).
26. Park, J. et al. New particle formation leads to enhanced cloud condensation nuclei concentrations on the Antarctic Peninsula. *Atmos. Chem. Phys.* **23**, 13625–13646 (2023).
27. Paglione, M. et al. Simultaneous organic aerosol source apportionment at two Antarctic sites reveals large-scale and ecoregion-specific components. *Atmos. Chem. Phys.* **24**, 6305–6322 (2024).
28. Dall'Osto, M. et al. Leaching material from Antarctic seaweeds and penguin guano affects cloud-relevant aerosol production. *Sci. Total Environ.* **831**, https://doi.org/10.1016/j.scitotenv.2022.154772 (2022).
29. Dall'Osto, M. et al. Sea Ice Microbiota in the Antarctic Peninsula Modulates Cloud-Relevant Sea Spray Aerosol Production. *Front. Marine Sci.* **9**, https://doi.org/10.3389/fmars.2022.827061 (2022).
30. Becagli, S. et al. Factors controlling atmospheric DMS and its oxidation products (MSA and nssSO42-) in the aerosol at Terra Nova Bay, Antarctica. *Atmos. Chem. Phys.* **22**, 9245–9263 (2022).
31. Bates, T. S., Calhoun, J. A. & Quinn, P. K. Variations in the methanesulfonate to sulfate molar ratio in submicrometer marine aerosol particles over the South Pacific Ocean. *J. Geophys. Res. Atmos.* **97**, 9859–9865 (1992).
32. Parkinson, C. & Cavalieri, D. Antarctic sea ice variability and trends, 1979-2010. *Cryosphere* **6**, 871–880 (2012).
33. Vichi, M. An indicator of sea ice variability for the Antarctic marginal ice zone. *Cryosphere* **16**, 4087–4106 (2022).
34. Kohout, A., Williams, M., Dean, S. & Meylan, M. Storm-induced sea-ice breakup and the implications for ice extent. *Nature* **509**, 604 (2014).
35. Alberello, A. et al. Brief communication: Pancake ice floe size distribution during the winter expansion of the Antarctic marginal ice zone. *Cryosphere* **13**, 41–48 (2019).
36. de Jager, W. & Vichi, M. Rotational drift in Antarctic sea ice: pronounced cyclonic features and differences between data products. *Cryosphere* **16**, 925–940 (2022).
37. Leng, C., Roberts, J., Zeng, G., Zhang, Y. & Liu, Y. Effects of temperature, pH, and ionic strength on the Henry's law constant of triethylamine. *Geophys. Res. Lett.* **42**, 3569–3575 (2015).
38. Fountoukis, C. & Nenes, A. ISORROPIA II:: a computationally efficient thermodynamic equilibrium model for K+-Ca2+-Mg2+-Nh4+-Na +-SO42–NO3–Cl–H2O aerosols. *Atmos. Chem. Phys.* **7**, 4639–4659 (2007).
39. Guo, H. et al. Fine-particle water and pH in the southeastern United States. *Atmos. Chem. Phys.* **15**, 5211–5228 (2015).
40. Guo, H. et al. Fine particle pH and the partitioning of nitric acid during winter in the northeastern United States. *J. Geophys. Res. Atmos.* **121**, 10355–10376 (2016).

41. Guo, H. et al. Fine particle pH and gas-particle phase partitioning of inorganic species in Pasadena, California, during the 2010 CalNex campaign. *Atmos. Chem. Phys.* **17**, 5703–5719 (2017).
42. Guo, H. et al. Effectiveness of ammonia reduction on control of fine particle nitrate. *Atmos. Chem. Phys.* **18**, 12241–12256 (2018).
43. Wiencke, C. & Amsler, C. D. *Seaweeds and Their Communities in Polar Regions*. 265–291 (Springer, 2012).
44. Amsler, C. et al. Comprehensive evaluation of the palatability and chemical defenses of subtidal macroalgae from the Antarctic Peninsula. *Mar. Ecol. Prog. Ser.* **294**, 141–159 (2005).
45. Otero, X., De La Peña-Lastra, S., Pérez-Alberti, A., Ferreira, T. & Huerta-Diaz, M. Seabird colonies as important global drivers in the nitrogen and phosphorus cycles. *Nat. Commun.* **9**, https://doi.org/10.1038/s41467-017-02446-8 (2018).
46. Riddick, S. et al. The global distribution of ammonia emissions from seabird colonies. *Atmos. Environ.* **55**, 319–327 (2012).
47. Fitzsimons, M., Tilley, M. & Cree, C. The determination of volatile amines in aquatic marine systems: a review. *Anal. Chim. Acta* **1241**, https://doi.org/10.1016/j.aca.2022.340707 (2023).
48. Gibb, S. & Hatton, A. The occurrence and distribution of trimethylamine-N-oxide in Antarctic coastal waters. *Mar. Chem.* **91**, 65–75 (2004).
49. Rocchi, A. et al. Distribution of alkylamines in surface waters around the Antarctic Peninsula and Weddell Sea. *Biogeosciences* **22**, 3429–3448 (2025).
50. Beale, R. & Airs, R. Quantification of glycine betaine, choline and trimethylamine N-oxide in seawater particulates: Minimisation of seawater associated ion suppression. *Anal. Chim. Acta* **938**, 114–122 (2016).
51. Lidbury, I., Murrell, J. & Chen, Y. Trimethylamine and trimethylamine N-oxide are supplementary energy sources for a marine heterotrophic bacterium: implications for marine carbon and nitrogen cycling. *ISME J.* **9**, 760–769 (2015).
52. Carpenter, L., Archer, S. & Beale, R. Ocean-atmosphere trace gas exchange. *Chem. Soc. Rev.* **41**, 6473–6506 (2012).
53. Chen, D. et al. Competitive uptake of dimethylamine and trimethylamine against ammonia on acidic particles in marine atmospheres. *Environ. Sci. Technol.* **56**, 5430–5439 (2022).
54. Chen, D. et al. Mapping gaseous dimethylamine, trimethylamine, ammonia, and their particulate counterparts in marine atmospheres of China's marginal seas - Part 1: Differentiating marine emission from continental transport. *Atmos. Chem. Phys.* **21**, 16413–16425 (2021).
55. Tian, R. et al. Freeze-thaw process boosts penguin-derived NH3 emissions and enhances climate-relevant particles formation in Antarctica. *NPJ Clim. Atmos. Sci.* **7**, https://doi.org/10.1038/s41612-024-00873-1 (2024).
56. Hoffmann, E., Tilgner, A. & Herrmann, H. An improved multiphase chemistry mechanism for methylamines: significant dimethylamine cloud production. *NPJ Clim. Atmos. Sci.* **7**, https://doi.org/10.1038/s41612-024-00665-7 (2024).
57. Mallet, M. et al. Biological enhancement of cloud droplet concentrations observed off East Antarctica. *NPJ Clim. Atmos. Sci.* **8**, https://doi.org/10.1038/s41612-025-00990-5 (2025).
58. Sanchez, K. et al. Measurement report: Cloud processes and the transport of biological emissions affect southern ocean particle and cloud condensation nuclei concentrations. *Atmos. Chem. Phys.* **21**, 3427–3446 (2021).
59. Niu, Q. et al. 62°S Witnesses the transition of boundary layer marine aerosol pattern over the Southern Ocean (50°S-68°S, 63°E-150°E) during the spring and summer: results from MARCUS (I). *J. Geophys. Res. Atmos.* **129**, https://doi.org/10.1029/2023JD040396 (2024).
60. Hu, Q. et al. Large increases in primary trimethylaminium and secondary dimethylaminium in atmospheric particles associated with cyclonic eddies in the Northwest Pacific Ocean. *J. Geophys. Res. Atmos.* **123**, 12133–12146 (2018).
61. Tao, Y., Liu, T., Yang, X. & Murphy, J. Kinetics and products of the aqueous phase oxidation of triethylamine by OH. *ACS Earth Space Chem.* **5**, 1889–1895 (2021).
62. Liu, C. et al. Ocean emission pathway and secondary formation mechanism of aminiums over the Chinese Marginal Sea. *J. Geophys. Res. Atmos.* **127**, https://doi.org/10.1029/2022JD037805 (2022).
63. van Pinxteren, M. et al. Aliphatic amines at the Cape Verde Atmospheric Observatory: Abundance, origins and sea-air fluxes. *Atmos. Environ.* **203**, 183–195 (2019).
64. Zhang, Q. et al. Contribution of marine biological emissions to gaseous methylamines in the atmosphere: An emission inventory based on multi-source data sets. *Sci. Total Environ.* **898**, https://doi.org/10.1016/j.scitotenv.2023.165285 (2023).
65. Ge, X., Wexler, A. & Clegg, S. Atmospheric amines - Part I. A review. *Atmos. Environ.* **45**, 524–546 (2011).
66. Almeida, J. et al. Molecular understanding of sulphuric acid-amine particle nucleation in the atmosphere. *Nature* **502**, 359 (2013).
67. Olenius, T. et al. New particle formation from sulfuric acid and amines: Comparison of monomethylamine, dimethylamine, and trimethylamine. *J. Geophys. Res. Atmos.* **122**, 7103–7118 (2017).
68. Zu, H., Chu, B., Lu, Y., Liu, L. & Zhang, X. Rapid iodine oxoacid nucleation enhanced by dimethylamine in broad marine regions. *Atmos. Chem. Phys.* **24**, 5823–5835 (2024).
69. Ge, X., Wexler, A. & Clegg, S. Atmospheric amines - Part II. Thermodynamic properties and gas/particle partitioning. *Atmos. Environ.* **45**, 561–577 (2011).
70. Jones, A. et al. Chemistry of the Antarctic Boundary Layer and the Interface with Snow: an overview of the CHABLIS campaign. *Atmos. Chem. Phys.* **8**, 3789–3803 (2008).
71. Draxler, R. & Hess, G. An overview of the HYSPLIT_4 modelling system for trajectories, dispersion and deposition. *Aust. Meteorol. Mag.* **47**, 295–308 (1998).
72. Carslaw, D. & Ropkins, K. openair - an R package for air quality data analysis. *Environ. Model. Softw.* **27-28**, 52–61 (2012).
73. Sandrini, S. et al. Size-resolved aerosol composition at an urban and a rural site in the Po Valley in summertime: implications for secondary aerosol formation. *Atmos. Chem. Phys.* **16**, 10879–10897 (2016).
74. Facchini, M. C. et al. Important source of marine secondary organic aerosol from biogenic amines. *Environ. Sci. Technol.* **42**, 9116–9121 (2008).
75. Seinfeld, J. H. & Pandis, S. N. *Atmospheric Chemistry and Physics: From Air Pollution to Climate Change*, 3rd edn. (John Wiley & Sons, 2016).
76. Decesari, S. et al. Source attribution of water-soluble organic aerosol by nuclear magnetic resonance spectroscopy. *Environ. Sci. Technol.* **41**, 2479–2484 (2007).
77. Decesari, S., Facchini, M., Fuzzi, S. & Tagliavini, E. Characterization of water-soluble organic compounds in atmospheric aerosol: a new approach. *J. Geophys. Res. Atmos.* **105**, 1481–1489 (2000).
78. Tagliavini, E. et al. Functional group analysis by HNMR/chemical derivatization for the characterization of organic aerosol from the SMOCC field campaign. *Atmos. Chem. Phys.* **6**, 1003–1019 (2006).
79. Weber, R., Guo, H., Russell, A. & Nenes, A. High aerosol acidity despite declining atmospheric sulfate concentrations over the past 15 years. *Nat. Geosci.* **9**, 282 (2016).
80. Bougiatioti, A. et al. Particle water and pH in the eastern Mediterranean: source variability and implications for nutrient availability. *Atmos. Chem. Phys.* **16**, 4579–4591 (2016).
81. Pye, H. et al. The acidity of atmospheric particles and clouds. *Atmos. Chem. Phys.* **20**, 4809–4888 (2020).
82. Song, S. et al. Fine-particle pH for Beijing winter haze as inferred from different thermodynamic equilibrium models. *Atmos. Chem. Phys.* **18**, 7423–7438 (2018).
83. Vasilakos, P., Russell, A., Weber, R. & Nenes, A. Understanding nitrate formation in a world with less sulfate. *Atmos. Chem. Phys.* **18**, 12765–12775 (2018).

84. Battaglia, M., Weber, R., Nenes, A. & Hennigan, C. Effects of water-soluble organic carbon on aerosol pH. *Atmos. Chem. Phys.* **19**, 14607–14620 (2019).
85. Akenga, P. & Fitzsimons, M. Automated method for the sensitive analysis of volatile amines in seawater. *ACS EST Water* **4**, 2504–2510 (2024).

Acknowledgements

The study was supported by the Spanish Ministry of Economy through project PI-ICE (CTM2017–89117-R) and the National Centre for Atmospheric Science funded by the Natural Environment Research Council. This work acknowledges the 'Severo Ochoa Centre of Excellence' accreditation (CEX2019-000928-S). Support from CleanCloud (Horizon Europe, grant no. 101137639) is also greatly acknowledged. The National Centre for Atmospheric Science (NCAS) Birmingham group is funded by the UK Natural Environment Research Council. We thank the Spanish Armada, and particularly the captains and crew of the BIO A-33 Hesperides, for their invaluable collaboration.

Author contributions

Conceptualization: M.D.O., M.P. Data Curation: M.D.O. and M.R. organized the field study. A.J. and T.L.C. obtained measurements at the BAS stations. A.S. obtained filter samples for water measurements. P.C.A. and M.F.F. carried out the water Alkylamines measurements. M.P., M.R. and S.D. carried out the atmospheric Alkylamines measurements. Software: D.C.S.B., J.B., K.M. Formal Analysis: D.C.S.B., M.D.O., M.P. Funding Acquisition: M.D.O., E.B., D.V. Methodology: D.C.B.S., J.B., M.P., K.M. Project Administration: M.D.O., M.P. Resources: M.D.O., E.B., D.V., M.P. Validation: All authors. Visualization: D.C.S.B., M.D.O. Writing: M.D.O., M.P. Review & Editing: All authors.

Competing interests

The authors declare no competing financial interests but the following Competing Non-Financial Interests: author R.M.H. is Editor-in-Chief of npj Climate and Atmospheric Science and was not involved in the journal's review of or decisions related to this manuscript.

Additional information

Supplementary information The online version contains supplementary material available at https://doi.org/10.1038/s41612-025-01284-6.

Correspondence and requests for materials should be addressed to Manuel Dall´Osto.